A Fully-Integrated W-Band I/Q-Down-Conversion MMIC for Use in Radio Astronomical Multi-Pixel Receivers

Fabian Thome[#1], Erdin Ture[#], Arnulf Leuther[#], Frank Schäfer[$], Alessandro Navarrini[*], Patrice Serres[^], and Oliver Ambacher[#]

[#]Fraunhofer IAF, Fraunhofer Institute for Applied Solid State Physics, Freiburg, Germany
[$]Max Planck Institute for Radio Astronomy, Bonn, Germany
[*]INAF (National Institute for Astrophysics)-Astronomical Observatory of Cagliari, Selargius (CA), Italy
[^]Institut de Radioastronomie Millimétrique (IRAM), Saint Martin d'Hères, France
[1]Fabian.Thome@iaf.fraunhofer.de

***Abstract* — In this paper, a W-band I/Q-down-conversion monolithic microwave integrated circuit (MMIC) is presented. The MMIC is based on the Fraunhofer IAF 50-nm gate-length metamorphic high-electron-mobility transistor technology and contains an RF 3-dB quadrature coupler, two subharmonically-pumped mixer cells, two IF low-noise amplifiers, and an LO chain including a frequency tripler, a band-pass filter, and two power amplifiers. The nonlinear circuits use an anti-parallel Schottky diode topology. The circuit covers an RF and IF bandwidth from at least 75 to 110 GHz and 3 to 13 GHz, respectively. The MMIC exhibits a single-sideband conversion gain of up to 17 dB and an average double-sideband noise figure in the range of 14.2–15.4 dB. The input-referred one-decibel compression point is up to −7 dBm. To the best of our knowledge, the presented W-band I/Q-down-conversion MMIC demonstrates state-of-the-art results with regards to complexity and performance.**

***Keywords* — High-electron-mobility transistors (HEMTs), I/Q-mixer, low-noise amplifiers (LNAs), millimeter wave (mmW), mixers, monolithic microwave integrated circuits (MMICs), radio astronomy, Schottky diodes, W-band.**

I. Introduction

Due to an atmospheric window, the W-band (75–110 GHz) frequency range attracts several applications, such as wireless communication, sensing, or imaging systems. Radio astronomy targets an even wider RF bandwidth. For example, the band 2 + 3 of the Atacama Large Millimeter Array aims at covering the 67–116-GHz range. In addition, systems in wireless communication and radio astronomy commonly require a large instantaneous RF bandwidth leading also to a large IF bandwidth while providing a sufficiently high sideband separation or sideband suppression. A major challenge for these systems is the combination of absolute performance parameters, such as a low system noise temperature, high RF and IF bandwidths, the avoidance of spurs, or a high return loss of the used components for the reduction of standing waves. State-of-the-art noise performance can be achieved by cryogenically-cooled low-noise amplifiers (LNAs) [1]. An RF amplification of more than 40 dB at the cryogenic stage offers the possibility to achieve an excellent receiver noise temperature while operating the RF downconverter at ambient temperature. Still, due to, e.g., large relative bandwidths at the RF, IF, and LO ports, a major part of the challenges remains for the down-conversion stage. An appealing example of a modular solution for such a down-conversion system is demonstrated in [2], covering an RF bandwidth from 67 to 116 GHz with an IF bandwidth from 4 to 12 GHz.

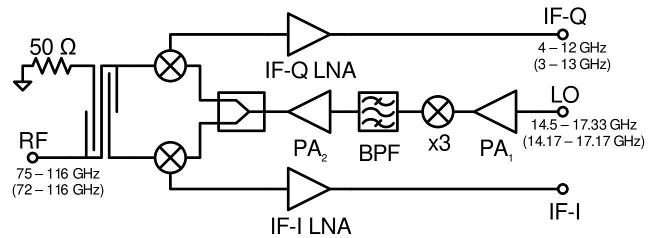

Fig. 1. Block diagram of the presented fully-integrated down-conversion MMIC. The baseline frequency ranges are depicted at the corresponding ports. In addition, the frequency goals are given in brackets.

A current trend, especially in radio astronomy, is the use of focal-plane arrays (FPAs) at the focus of radio telescopes in order to improve the survey speed during observations of extended radio astronomy sources. However, in addition to the existing challenges for such receiver systems, FPAs put a serious constraint on the distance between neighboring pixels and by that on the integration density of each pixel. The spacing is primarily defined by the optics of a radio telescope. In [3], a 16-pixel array is demonstrated for an RF bandwidth from 85 to 116 GHz where each pixel is based on a hybrid integration of several monolithic microwave integrated circuits (MMICs) in a single split-block module.

In this work, we target a further improvement of the integration density by combining major parts of the RF down-conversion on a single MMIC. Therefore, we demonstrate an I/Q-down-conversion circuit which is based on the Fraunhofer IAF 50-nm gate-length InGaAs metamorphic high-electron-mobility transistor (mHEMT) technology. The MMIC contains an RF 3-dB quadrature coupler, two subharmonically-pumped mixer cells, two IF LNAs, and an LO chain including a frequency tripler (x3), a band-pass filter, and two power amplifiers (PAs). For an improved system noise temperature, the RF LNAs are cryogenically cooled and provide a gain of 40 to 50 dB. Thus, the presented down-conversion MMIC does not include a room-temperature RF LNA.

II. W-Band Down-Conversion MMIC

The presented fully-integrated down-conversion MMIC has the following requirements. Firstly, the baseline frequency

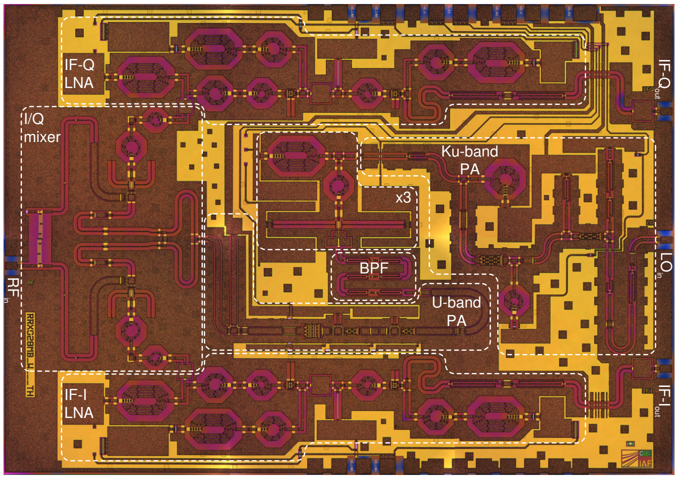

Fig. 2. Photograph of the fabricated fully-integrated down-conversion MMIC. The chip has a size of $4.25 \times 3\,\mathrm{mm}^2$.

ranges are (goal values are given in brackets): RF 75–116 GHz (72–116 GHz) and IF 4–12 GHz (3–13 GHz). Secondly, the MMIC aims to be pumped by a frequency-tunable LO tone in the approx. 14–18-GHz range (to be discussed further down). The LO steps within the LO frequency range to cover the entire RF range with the given IF bandwidth. Thirdly, the down-conversion MMIC should enable a receiver with a sideband-separating approach. Thus, an I/Q-mixer topology is required. Fourthly, to avoid interference issues of the LO signal at the IF outputs, the LO input frequencies should be outside the IF range which means above 13 GHz, but should be below 20 GHz. Therefore, a multiplication factor of the LO frequencies of six is needed. This can be realized, e.g., by an LO chain with a multiplication factor of six or by an x3 in combination with a subharmonically-pumped mixer. In this work, the latter of which was chosen. Compared to a frequency multiplier by six (x6), an x3 is easier to realize in a fully-integrated down-conversion MMIC. This is, due to filtering reasons, especially the case when targeting fairly wideband multipliers. Furthermore, an x6 would require either a direct multiplication by six which is, in general, considerably inefficient, or two multiplication stages which increases the occupied chip area and makes the filtering and avoidance of spurs even more challenging. A block diagram of the presented fully-integrated down-conversion MMIC is illustrated in Fig. 1. To obtain a maximum of isolation between the individual building blocks while still achieving a considerably compact layout, each sub-circuit is designed in a grounded-coplanar waveguide environment.

The mixer cells and the x3 are based on an anti-parallel Schottky diode topology. The diodes feature a Schottky contact with a size of $0.25 \times 4\,\mu\mathrm{m}^2$ each and use the same process flow so that diodes and HEMT are simultaneously available. Each nonlinear circuit utilizes eight diodes. The mixer cell contains dedicated filter networks at all ports to improve the isolation of the ports to each other. Based on measurements of a test structure, the single-sideband conversion gain (CG_{SSB}) of the mixer cell is about −12 to −11 dB while covering at least the

Table 1. Bias of the MMIC at the DC Pads

	IF LNAs	PA$_1$	PA$_2$		x3
V_d	0.86 V	1.2 V	1.7 V	V_{x3}	2 V
I_d	83.5 mA	217 mA	312 mA		

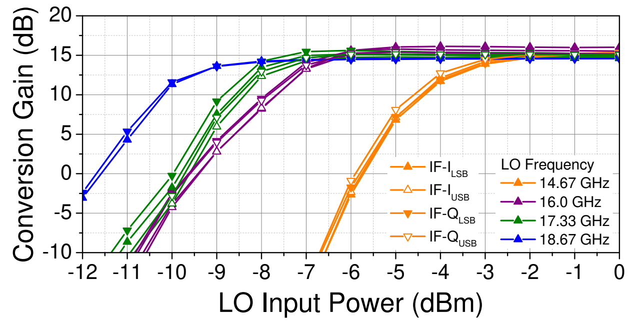

Fig. 3. Measured CG_{SSB} as a function of LO input power for four different LO frequencies. The IF is 4 GHz. The RF input power is −25 dBm. LSB and USB are illustrated by closed and open symbols, respectively.

W-band frequency range with an IF of at least 0–15 GHz.

At the RF input of the fully-integrated MMIC, a Lange coupler is used as 3-dB quadrature coupler. From 66 to 118 GHz, the coupler exhibits a measured amplitude and phase imbalance of less than ±0.5 dB and ±1°, respectively. Measurements of an I/Q-mixer test structure, including a Lange coupler, two mixer cells, and a Wilkinson splitter, demonstrate a CG_{SSB} in the range of −16 to −14 dB which corresponds to the expectations. Each IF path comprises a two-stage LNA with a $4 \times 35\,\mu\mathrm{m}$ HEMT per stage. To prevent issues with standing waves, specific attention was paid to the input and output return loss of the LNAs. Therefore, especially the first stage feature an inductive source degeneration to obtain good simultaneous input noise and power matching. The LNA is designed for a frequency range from 3 to 13 GHz. Based on simulations, a flat noise figure of below 1 dB is expected, which enables an overall flat noise performance of the entire down-conversion MMIC. The simulated gain of the LNA is 27–31 dB (with a falling slope towards higher frequencies).

The central building block of the LO chain is the x3 which can be biased so that the output power can be adjusted between −8 and 0 dBm with almost constant conversion efficiency. Due to the anti-parallel diode topology, even harmonic frequencies can be expected to be well suppressed. Thus, the filtering of unwanted harmonics has to focus mainly on the fundamental and the fifth harmonic. Therefore, a band-pass filter is integrated after the x3 which lowers the fundamental by at least 30 dB and the fifth harmonic by approximately 5 dB. At the LO input, a PA (PA$_1$) is used to drive the x3. It is a two-stage amplifier with a $4 \times 125\,\mu\mathrm{m}$ HEMT in the first stage and a $6 \times 125\,\mu\mathrm{m}$ HEMT in the second stage. PA$_1$ can deliver an output power of 16–18 dBm while requiring an input power of up to 0 dBm. PA$_2$ amplifiers the output signal of the x3 and provides the LO drive power for the I/Q-mixer. PA$_2$ uses three stages with $4 \times 65\,\mu\mathrm{m}$ HEMTs in the first two stages and a $8 \times 80\,\mu\mathrm{m}$

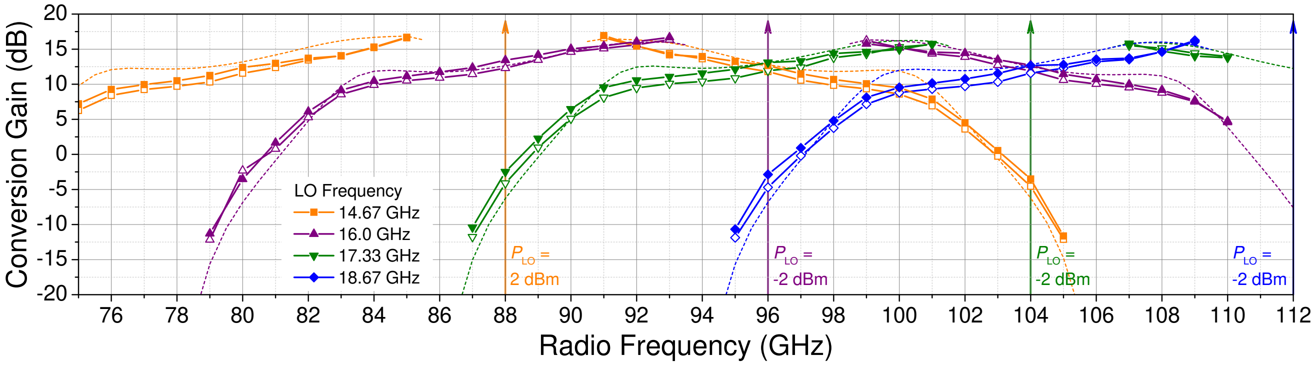

Fig. 4. Measured (symbols) and simulated (dashed lines) single-sideband conversion gain as a function of radio frequency. CG_{SSB} of LSB and USB is measured for four different LO input frequencies and a fixed-LO scenario. The data for the I and Q path of the MMIC are given in closed and open symbols, respectively. As indication for the LO, arrows illustrate the sixfold LO input frequency. P_{LO} is given at the corresponding arrow. The RF input power is −25 dBm.

Table 2. Summary of MMIC Measurements

LO Freq. (GHz)	SSB Conversion Gain vs. RF: I LSB (dB)	Q LSB (dB)	I USB (dB)	Q USB (dB)	Avg. DSB NF: I (dB)	Q (dB)
	Baseline: 4–12 GHz					
14.67	9.3–15.2	8.4–15.3	9.5–15.5	8.6–15.4	14.8	15.3
16	10.5–16.1	9.9–15.6	9.2–15.2	8.8–15.2	14.2	15.2
17.33	10.6–15	9.5–15.3	13.8–14.7*	14–15.1*	14.2*	15.1*
18.67	9.6–14.6	8.8–14.6	n/a*	n/a*	n/a*	n/a*
	Goal: 3–13 GHz					
14.67	7.3–16.6	6.3–17	7.9–16.9	6.9–16.6	14.8	15.4
16	9.1–16.7	8.5–16.3	7.7–15.8	7.5–16.2	14.2	15.2
17.33	9.5–15.8	8.1–15.7	13.8–15.8*	14–15.5*	14.2*	15.2*
18.67	8.1–16.1	7.2–16.3	n/a*	n/a*	n/a*	n/a*

* Measured frequency range limited by measurement setup.

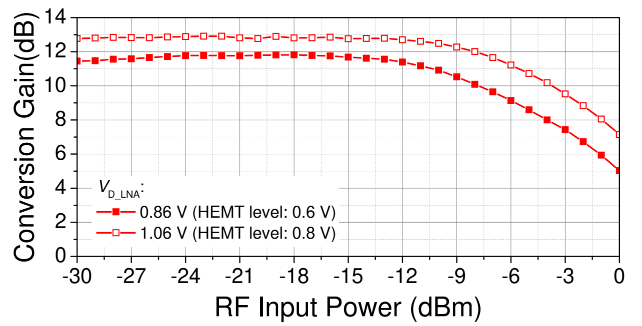

Fig. 5. Measured CG_{SSB} as a function of RF input power. The RF and LO input frequencies are at 97 and 17.5 GHz, respectively. Thus, the LSB is measured with an IF of 8 GHz. The LO input power is −2 dBm.

HEMT in the output stage. With an input power of 0 dBm, the amplifier can deliver 16–17 dBm at the output. Further details about the sub-circuits are discussed in [4]. In Fig. 2, a photograph of the fabricated fully-integrated W-band down-conversion MMIC is depicted.

III. Measurement Results

The MMIC was measured on wafer with two different setups. First the conversion gain was measured for different scenarios. In a second step, the double-sideband (DSB) noise figure (NF) was characterized. Unless otherwise stated, the bias of the MMIC was for all measurements identical and is summarized in Table 1. The total power consumption of the MMIC is about 870 mW.

A. Conversion Gain

The RF input signal is provided by a signal generator, a frequency multiplier by six, and a motorized waveguide attenuator. The multiplier limits the RF range to frequencies from 75 to 110 GHz. The LO input signal is provided by a second signal generator. The IF output signal is measured by a Keysight signal analyzer. The input and output signals are calibrated to the RF probe tips. While measuring an IF output, a termination is connected to the second IF output. For all measurements, the given values for the conversion gain are single-sideband parameters.

In Fig. 3, CG_{SSB} is shown as a function of LO input power (P_{LO}) for LO frequencies of 14.67, 16, 17.33, and 18.67 GHz and for the lower sideband (LSB) and upper sideband (USB), respectively. For the higher LO frequencies, the conversion gain saturates for a power level of more than −5 dBm. For the lowest LO frequency, an LO input power of more than −1 dBm is required. In saturation, CG_{SSB} is for all measured combinations within 14.6–16 dB. For the same LO frequencies, the measured CG_{SSB} is shown as a function of RF in Fig. 4. The performance is summarized in Table 2 for IF-I and IF-Q as well as for LSB and USB. The MMIC exhibits a good conversion gain for the aimed IF range from 3 to 13 GHz with a difference between the sidebands and IF paths of less than 1 dB over most parts of the band. Even in extreme cases, the difference is below 1.7 dB. At the lower IF band edge, the conversion gain achieves values of 16–17 dB.

The compression behavior versus RF input power is depicted in Fig. 5. For the standard bias ($V_{\mathrm{D\_LNA}} = 0.86\,\mathrm{V}$), the input power for one-decibel compression ($P_{1\,\mathrm{dB}}$) is −9.5 dBm and can be increased to −7 dBm if the IF LNAs are biased with a drain voltage of 1.06 V.

A wafer mapping including 22 working cells out of 37 cells on a wafer is shown in Fig. 6. Considering the complexity of the MMIC, a good yield is demonstrated. The variation of the average conversion gain between the different cells is below 2 dB. It is important to mention that the mapping was done

Table 3. State-of-the-Art W-Band Down-Conversion MMICs

Ref.	Technology	Topology	RF (GHz)	LO Freq. (GHz)	IF (GHz)	CG_{SSB} (dB)	$P_{1\,\mathrm{dB}}$ (dBm)	DSB NF (dB)
[5]	65-nm CMOS	single-ended (RF LNA, mixer, IF amp.)	75–91	89	1–9	14.5–16.5	−16.2	7–9
[6]	90-nm CMOS	single-ended (RF LNA, x3, mixer, IF amp.)	78–105	26	0–27	≈0	n/a	17–20
[7]	65-nm CMOS	single-ended (RF LNA, x3, mixer, IF amp.)	77–110	28–36	0–31	4–20	−20/−15	17–27
This work	50-nm mHEMT	I/Q (I/Q-mixer, IF LNA, x3, PAs)	75–110	14.67–18.67	4–12 (3–13)	8.4–16.1 (6.3–17)	−9.5/−7	14.2–15.3 (14.2–15.4)

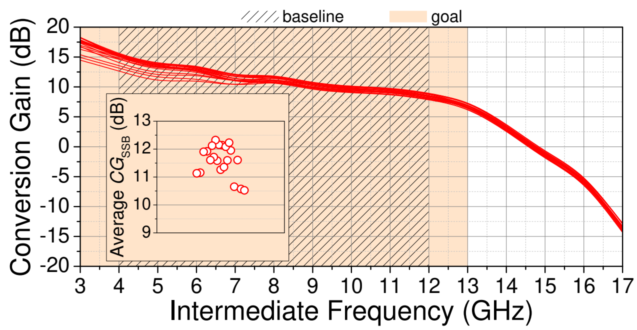

Fig. 6. Wafer mapping including 22 measured cells out of 37 cells on a wafer. CG_{SSB} is shown for the USB and a fixed LO frequency and LO input power of 15.5 GHz and −2 dBm, respectively. The insert shows a scatterplot of the average conversion gain (averaged from 4 to 12 GHz).

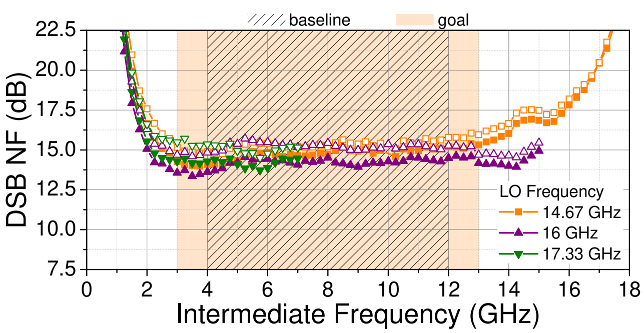

Fig. 7. Measured double-sideband noise figure as a function of intermediate frequency for three LO frequenies in the W-band RF range. The LO input power is similar as in Fig. 4. The data for the I and Q path of the MMIC are given in closed and open symbols, respectively.

with a constant bias. An individualized bias for each cell might further improve the homogeneity of the measured MMICs.

B. DSB Noise Figure

The noise performance was characterized with an on-wafer setup which is comparable to the one in Section III-A. At the RF input port, an ELVA-1 WR10 waveguide noise source is used. The noise source is calibrated for a frequency range from 70 to 111 GHz. The IF output signal is measured with a Keysight noise figure analyzer. The measured DSB noise figure is illustrated in Fig. 7 as a function of IF for the corresponding RF range, which is determined by the calibrated frequency range of the noise source. The noise figure shows a flat performance for an IF from at least 3 to 13 GHz. The average DSB NF is summarized in Table 2 and is between 14.2 and 15.4 dB for all measured combinations. When biased for improved $P_{1\,\mathrm{dB}}$ ($V_{\mathrm{D\_LNA}} = 1.06\,\mathrm{V}$), the measured DSB NF is about 0.1 dB higher.

IV. Discussion and Conclusion

In this paper, a fully-integrated W-band I/Q-down-conversion MMIC is demonstrated in the Fraunhofer IAF 50-nm gate-length mHEMT technology. The MMIC contains an RF 3-dB quadrature coupler, two subharmonically-pumped mixer cells, two IF LNAs, and an LO chain including a frequency tripler, a band-pass filter, and two PAs. The measurements exhibit a single-sideband conversion gain of up to 17 dB and an average double-sideband noise figure in the range of 14.2–15.4 dB while covering an RF and IF bandwidth of at least 75–110 GHz and 3–13 GHz, respectively. Table 3 summarizes previously published MMICs that, however, demonstrate only single-ended performance. It is important to mention that the given references contain an RF LNA which, on the one hand, mainly determines the noise performance and, on the other hand, commonly limits $P_{1\,\mathrm{dB}}$. To the best of our knowledge, this work demonstrates the best I/Q-downconverter in W-band that is realized on a single MMIC at this integration level in combination with the obtained noise performance, $P_{1\,\mathrm{dB}}$, and RF and IF bandwidth. The achieved results are appealing for multi-pixel receiver systems in radio astronomy and other highly-integrated wideband applications.

Acknowledgment

The authors thank the colleagues at Fraunhofer IAF for their excellent contributions during epitaxial growth and wafer processing. The authors also thank S. Wagner for supporting the RF measurements. This project has received funding from the European Union's Horizon 2020 research and innovation programme under grant agreement No 730562.

References

[1] F. Thome *et al.*, "70–116-GHz LNAs in 35-nm and 50-nm Gate-Length Metamorphic HEMT Technologies for Cryogenic and Room-Temperature Operation," in *IEEE MTT-S Int. Microw. Symp.*, Jun. 2018, pp. 1495–1498.

[2] B. Thomas *et al.*, "A dual-polarization sideband separating Schottky based receiver for ALMA Band 2+3 Warm Cartridge Assembly," in *Int. Symp. Space THz Technol.*, Mar. 2018, pp. 95–97.

[3] M. Sieth *et al.*, "Argus: a 16-pixel millimeter-wave spectrometer for the Green Bank Telescope," in *SPIE Astron. Telescopes Instrum.*, vol. 9153, Jul. 2014, pp. 1–12.

[4] F. Thome *et al.*, "Frequency Multiplier and Mixer MMICs Based on a Metamorphic HEMT Technology Including Schottky Diodes," *IEEE Access*, vol. 8, pp. 12 697–12 712, 2020.

[5] M. Khanpour *et al.*, "A Wideband W-Band Receiver Front-End in 65-nm CMOS," *IEEE J. Solid-State Circuits*, vol. 43, no. 8, pp. 1717–1730, Aug. 2008.

[6] J. J. Yu, C. Liao, C. Hsieh, R. Hu, and D. Niu, "77–110GHz 90nm-CMOS receiver design," in *Asia–Pacific Microw. Conf.*, Nov. 2013, pp. 233–235.

[7] C.-Y. Huang, K.-L. Wu, R. Hu, and C.-Y. Chang, "Analysis of wide- IF-band 65 nm-CMOS mixer for 77–110 GHz radio-astronomical receiver design," *IET Circuits Devices Syst.*, vol. 13, pp. 406–413, May 2019.